Granger causality analysis of functional connectivity of spiking neurons in orofacial motor cortex during chewing and swallowing

Kazutaka Takahashi, Lorenzo Pesce, José Iriarte-Díaz, Sanggyun Kim,
Todd P. Coleman, Nicholas G. Hatsopoulos, and Callum F. Ross

Abstract—Primate feeding behavior is characterized by a series of jaw movement cycles of different types making it ideal for investigating the role of motor cortex in controlling transitions between different kinematic states. We recorded spiking activity in populations of neurons in the orofacial portion of primary motor cortex (MIo) of a macaque monkey and, using a Granger causality model, estimated their functional connectivity during transitions between chewing cycles and from chewing to swallowing cycles. We found that during rhythmic chewing, the network was dominated by excitatory connections and exhibited a few "out degree" hub neurons, while during transitions from rhythmic chews to swallows, the numbers of excitatory and inhibitory connections became comparable, and more "in degree" hub neurons emerged. These results suggest that networks of neurons in MIo change their operative states with changes in kinematically defined behavioral states.

I. INTRODUCTION

Primate feeding behavior is characterized by a series of cycles of different types–ingestion, manipulation, chewing, swallowing [1]. Previous studies employing single electrode recording techniques [2], [3] have shown that majority of neurons in MIo show activity related to rhythmic chewing, preswallowing and/or swallowing. In this study, we simultaneously recorded jaw kinematics and spiking activity of neuronal ensemble in the orofacial area of MI, and estimated changes in the network of spiking neurons during transitions between different kinematic states.

II. METHOD

A. Behavior task and data collection

All of the surgical and behavior procedures were approved by the University of Chicago IACUC and conform to the principles outlined in the Guide for the Care and Use of Laboratory Animals. One female macaque monkey was trained to feed with her right hand while restrained in a primate chair. Her head was restrained with a halo coupled to the cranium through chronically implanted headposts. Detailed methods of collecting jaw kinematic data are described in

detail elsewhere [4], [5]. Three dimensional jaw kinematic data were collected in the coordinate system of the cranium using an infrared light video-based motion analysis system (Vicon Motion Tracking System with 10 MX 40 cameras with sampling rate of 250 Hz) which tracked reflective markers coupled to the mandible and cranium using bone screws. The marker coordinates were bi-directionally low-pass filtered with a 4th order Butterworth filter with 15 Hz cutoff frequency.

Using movements of the mandibular marker, jaw movement cycles were defined by two consecutive maximum gapes (i.e., maximum open). The cycles in each feeding sequence were then assigned into five different cycle types: ingestion, manipulation, stage-1 transport, rhythmic chew and swallow [1]. In this study, we focused on transitions between two consecutive rhythmic chew cycles (Chew Transitions) and between rhythmic chewing and swallow cycles (Swallow Transitions). 94.4% of chew cycle durations were shorter than 600 ms, with the mode and mean being approximately 300 ms. Thus 300 ms was used to represent a canonical duration of one chew cycle for the rest of the study.

We recorded multiple single unit spiking activities from a chronically implanted 100-electrode Utah microelectrode array (1.5 mm in length, 10 x 10 grid, 400 μm interelectrode spacing, Blackrock Microsystems, Utah, USA,) in the oro-facial area of primary motor cortex (MIo) on the left side of the monkey. Spiking activities from up to 96 channels were recorded at 30 kHz. Spike waveforms were sorted offline using a semiautomated method incorporating a previously published algorithm [6]. The signal to noise ratio (SNR) for each unit was defined as the difference in mean peak to trough voltage divided by twice the mean standard deviation computed from all the spikes at each sample points. All the units with SNR< 3 were discarded for the current study. The data for each neuron were converted to a binary time series with 1 ms temporal resolution over a window of [-300, 300] ms centered on the maximum gape [0]ms separating either two chewing cycles (Chew Transitions, 833 events), or a Chew and swallow cycle (Swallow Transitions, 65 events). Among neurons available for analysis, we used 71 neurons whose mean spike rates over the time window of interest exceeded 2 spikes/sec. Then, for each type of transition, the data were further divided into three Time Windows: 1 for [-300, 0], 2 for [-150, 150], and 3 for [0,300] ms.

B. Analysis

A neural spike train is modeled as a point process [7], [8], which is characterized by its conditional intensity function (CIF), $\lambda(t|H(t))$, where $H(t)$ denotes the spiking history of all neurons in the ensemble up to time t. In the generalized linear model (GLM) framework, the log CIF was modeled as a linear combination of the covariates, $H(t)$, which describes the neural activity dependencies [9]. Thus the logarithm of the CIF for neuron i is expressed by

$$\log \lambda_i(t|\boldsymbol{\theta}_i, H(t)) = \theta_{i,0} + \sum_{n=1}^{N} \sum_{m=1}^{M_i} \theta_{i,n,m} R_{n,m}(t), \quad (1)$$

where $\theta_{i,0}$ relates to a background level of activity, and $\theta_{i,n,m}$ represents the effect of ensemble spiking history $R_{n,m}(t)$ of neuron n on the firing probability of neuron i at time t for $n = 1, ..., N$ neurons. In this work, we denote the spike count of neuron n in a time window of length W covering the time interval $[t-mW, t-(m-1)W]$ as $R_{n,m}(t)$ for $n = 1, ..., N$ and $m = 1, ..., M_i$. In this analysis we intuitively set W to 3 ms to obtain a relatively small number of parameters while maintaining the necessary temporal resolution. In order to select a model order, M_i, for each neuron i we fit several models with different history durations $M_i W$ to each spike train and then identified the best approximating model from among a set of candidates using Akaike's information criterion (AIC) [10], [11]. Using this criterion, an optimum model order for each neuron was selected to minimize the criterion. For each neuron M_i were ranged from 1 to 20 in our analysis.

Recently a point process framework for assessing causal relationship between neurons was proposed in [12]. Based on Granger's definition of the causality [13], a potential causal relationship from neuron j to i can be assessed based on the log-likelihood ratio given by

$$\Gamma_{ij} = \log \frac{\Pr(\text{future of } i|\text{past of everyone})}{\Pr(\text{future of } i|\text{past of everyone except } j)}. \quad (2)$$

If past values of neuron j contain information that helps predict future values of neuron i, the log likelihood ratio of (2), Γ_{ij}, is greater than zero. The equality of Γ_{ij} to zero holds when neuron j has no causal influence on i. This statistical framework for assessing Gragner causality can be applied to any modality as well as binary neural spike train data [14].

In summary, the Granger causality from neuron j to i is identified in the following way. First, the point process likelihood function of neuron i, denoted by $L_i(\boldsymbol{\theta}_i|H(t))$, is calculated using the parametric CIF of (1); It relates the ith neuron's spiking probability to possible covariates such as its own spiking history as well as the concurrent activity of other simultaneously recorded neurons [9]. Next, we assess the causal relationship from neuron j to i by calculating the relative reduction in the likelihood of neuron i obtained by excluding the covariate effect of neuron j (spiking history of neuron j) compared to the likelihood obtained using all the covariates, (spiking history of all neurons). The log-

likelihood ratio, Γ_{ij}, is given by

$$\Gamma_{ij} = \log \frac{L_i(\boldsymbol{\theta}_i)}{L_i(\boldsymbol{\theta}_i^j)}, \quad (3)$$

where the parameter vector $\boldsymbol{\theta}_i^j$ is obtained by re-optimizing the parametric likelihood model after excluding the effect of neuron j. Since the likelihood $L_i(\boldsymbol{\theta}_i)$ is always greater than or equal to the likelihood $L_i(\boldsymbol{\theta}_i^j)$, the log-likelihood ratio Γ_{ij} is always greater than or equal to 0. If the spiking activity of neuron j has a causal influence on that of neuron i in the Granger sense, the likelihood $L_i(\boldsymbol{\theta}_i)$ is greater than $L_i(\boldsymbol{\theta}_i^j)$. The equality holds when neuron j has no influence on i. The Granger causality measure given by (3) provides an indication of the extent to which the spiking history of neuron j affects the spike train data of neuron i, but little insight into which of these interactions are statistically significant. To address this issue, multiple hypothesis testing was performed based on the likelihood ratio test statistic [15],[16]. Thus, we can construct two $N \times N$ causality matrices, whose (i,j)th element represents the relative causality strength from neuron j to i; and corresponds to either statistically significant or insignificant interaction, respectively. Excitatory and inhibitory influences of neuron j on neuron i can be distinguished by the sign of $\sum_{m=1}^{M_i} \theta_{i,j,m}$ that represents an averaged influence of the spiking history of neuron j on neuron i.

Once the causality matrix was obtained for each data set, degrees for each neuron that showed any statistically significant interactions ($p < 0.005$) were computed. A degree of neuron i was defined as the number of neurons that are connected to neuron i by at least one interaction [17]. Since the resultant networks are bidirectional graphs, both in-degrees (number of connections made into a neuron) and out-degrees (number of connections made out of a neuron) were examined per each Time Window under each transition. Due to the high demand on CPU time, it was not feasible to perform calculations on a PC or a small cluster environment. MATLAB codes were modified from those used in [18], compiled, and run as the executables distributedly on the Cray machine, Beagle.

III. RESULTS

Sets of causality networks of 71 spiking neurons were obtained for the Chew and Swallow Transitions over different Time Windows using the method in [12]. Fig. 1 (a) shows the kinematic traces of the mandibular marker during consecutive chew cycles (Chew Transition in green), or consecutive Chew and Swallow cycles (Swallow Transition in yellow). Those two traces are remarkably similar during the chew cycle prior to the transition (maximum gape), but diverge during the swallow, which is characterized by a long slow open phase of the gape cycle. Fig. 1 (b), (c), and (d) show the statistically significant causal interactions ($p < 0.005$) for Chew Transitions at three different times relative to the maximum gape (at 0 ms) between two consecutive cycles: Time Window 1 was from $[-300, 0]$ ms, Time Window 2 was from $[-150, 150]$ ms, and Time Window 3 was from $[0, 300]$
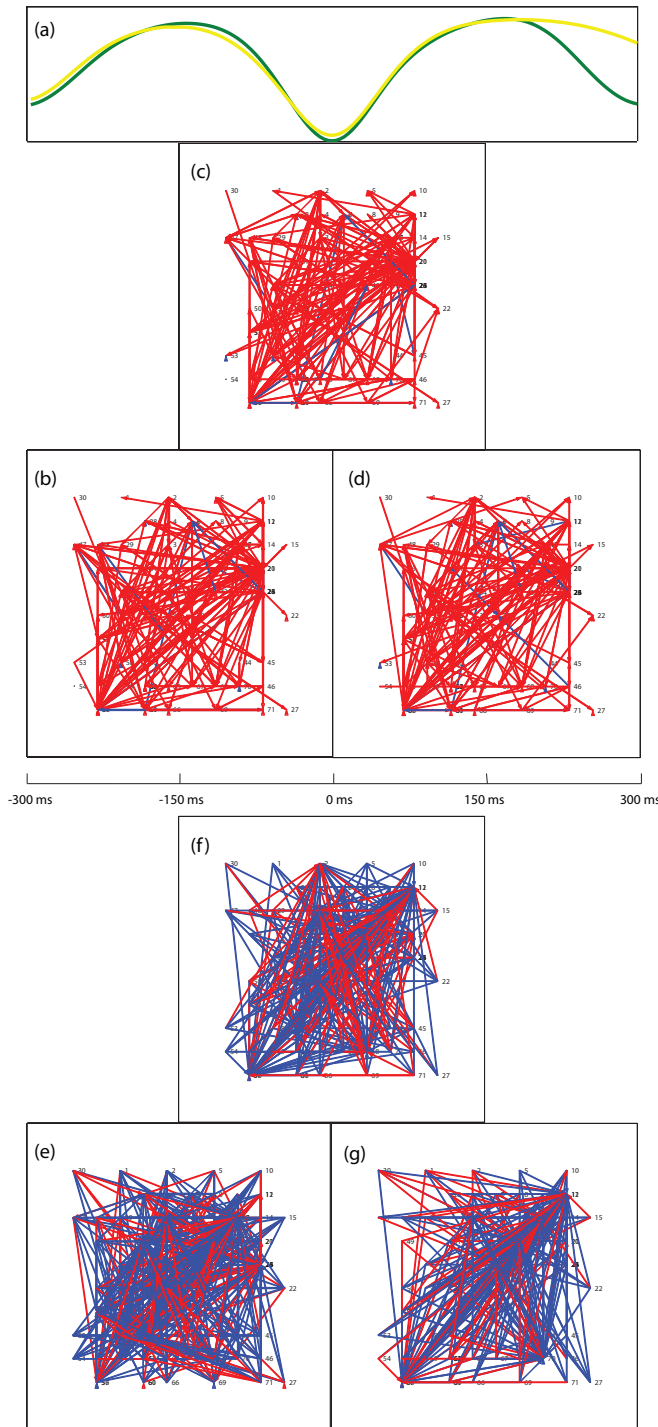
Fig. 1. Causality networks estimated in different Time Windows relative to the maximum gape between two consecutive cycles. (a) Mandibular marker trajectories for Chew Transition in yellow and Swallow Transition in green. (b∼d): Causality networks estimated at different times relative to maximum gape at 0 ms. Left column for Time Window [−300, 0] ms, middle column [−150, 150], and right column [0, 300] ms. Each dot indicates a neuron at a location on the array of the electrode that recorded that neuron. The location of the array is such that the upper right corner corresponds to caudomedial and the right edge roughly aligns to the central sulcus. Red lines indicate excitatory connections while blue lines inhibitory connections. (b)∼(d) for Chew Transitions show predominantly excitatory connections; (e)∼(g) for Swallow Transitions show more balanced numbers of excitatory and inhibitory connections, and slightly fewer connections.

ms. (e), (f), and (g) show the statistically significant causal interactions ($p < 0.005$) for Swallow Transitions at the same Time Windows as in (b),(c), and (d) respectively. As shown in (b)∼(d), the majority of the connections is excitatory during Chew Transitions, while in (e)∼(g), more inhibitory connections are present during Swallow Transitions. Gross connection topology did not change as much as the results seen in spiking neuron networks from the arm area of MI around visual cues [18]; rather within each transition connection patterns appeared to be fairly similar over the three Time Windows.
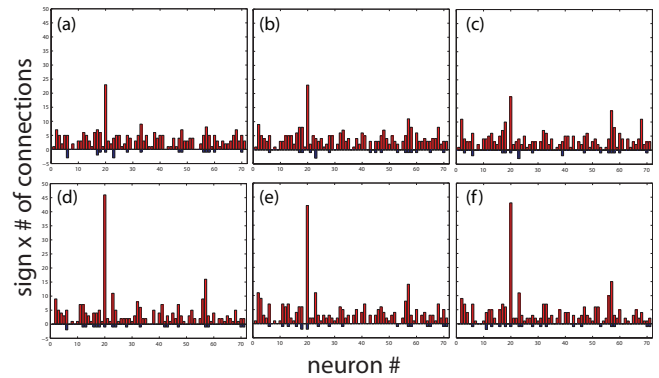

Fig. 2. The in- and out-degrees of all neurons obtained from all three Time Windows for Chew Transitions. Top: (a)∼(c) show in-degrees of all neurons from Time Windows 1, 2, and 3 respectively . Bottom: (d)∼(f) show out-degree of all neurons from Time Windows 1, 2, and 3 respectively.In each window, a red bar indicates a number of excitatory degree while a blue bar indicates a number of inhibitory degree multiplied by −1 for a neuron. Neuron #20 is a dominant hub neuron in this transition, especially in out-degree.

Fig. 2 shows in- and out-degree counts of each neuron for each Time Window for Chew transition. As seen in Fig. 1, excitatory connections are dominant, and in-degree and out-degree patterns are fairly similar across all three Time Windows. Neuron # 20 shows an unusually high degree, both in and out, of excitatory interactions across all Time Windows. Neuron #57 is the second largest hub in out-degree across all Time Windows, while in in-degree, the number of incoming connections for the neuron increases as the cycles progress from one rhythmic chew to the next.

Fig. 3 shows in- and out-degree counts for each Time Window for Swallow Transition. Unlike Fig. 2, inhibitory connections are more prominent than the excitatory counterparts for both in- and out-degrees, but a striking difference between those two types of degrees is that there is only a small fraction of neurons that show non-zero and high in-degrees, while all neurons examined here have non-zero and small out-degrees. Thus, only in-degree hub neurons exist in this transition. Furthermore, those hub neurons dynamically change during a transition from a rhythmic chew cycle to a swallow cycle.

IV. DISCUSSIONS

Primates intercalate swallows into chewing sequences [19]. Previous studies [2], [3] have shown that the majority
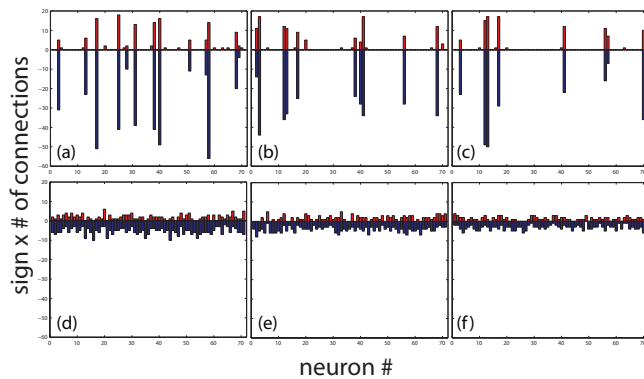
Fig. 3. The in- and out-degrees of all neurons obtained from all three Time Windows for Swallow Transition. Top: (a)∼(c) show in-degrees of all neurons from Time Windows 1, 2, and 3 respectively. Bottom: (d)∼(f) show out-degree of all neurons from Time Windows 1, 2, and 3 respectively. Plotting scheme here is the same as that in Fig. 2. More excitatory connections in and out of neurons than the Chew Transition. In-degrees and out-degrees exhibit different patterns for this transition. Only a fraction of neurons receive inputs from other neurons while most neurons are making a few number of connections outward.

of neurons in MIo show activity related to rhythmic chewing, preswallowing and/or swallowing, suggesting that primate MIo may play a critical role in the regulation of mastication, swallowing, and transitioning between the two. Yao et al. [2] showed that a subset of neurons exhibiting chewing related activities was also modulated in relation to swallow of solid foods or juice rewards. Furthermore, simple properties of single unit spike rates such as peak firing frequency did not show significant differences over chewing or swallow cycles. Yamamura et al. [3] showed that inactivation of MIo affected preswallow activity, but not swallow activity itself in terms of EMG parameters. Thus, in addition to continuously monitoring jaw and tongue kinematics during feeding behavior, neurons in MIo may pay attention to state transitions from rhythmic chewing to swallowing.

In order to investigate whether we can detect changes in networks of spiking neurons associated with states during feeding, we looked specifically at Chew Transition and Swallow Transition using a Granger causality measure for point process models [12] applied to multiple spike trains recorded from MIo. Our results reveal that two completely different types of causal networks during chewing and swallowing. During Chew Transitions, the majority of neurons is interacting with each other via excitatory connections with a few hub neurons with very high in- and out-degrees. In contrast, during Swallow Transitions, inhibitory connections are more common and in- and out-degree patterns are asymmetric: The majority of neurons exhibits a small number of out-degrees, while only a small fraction of neurons receives inputs at all from other neurons. Different neurons form in-degree hubs at different Time Windows. Thus the current analysis illustrates time- and state-dependent functional effects of single MIo neuron on other neurons and how network topology changes across kinematic state transitions.

Furthermore, as Fig. 3 (a) and (d) show, the network

structure during a rhythmic chew cycle prior to the transition to a swallow cycle is already completely different from that during continuation of rhythmic chew cycles. This implies that MIo changes network connectivity in anticipation of a swallow at least one cycle earlier than the swallow actually occurs. This study was limited only to neurons from MIo, but clearly feeding behavior involves a very complex sensory-motor interactions. Therefore, in order to further increase our understanding of complex sensory-motor behaviors such as feeding, we should look at properties of networks of spiking neurons.

REFERENCES

[1] A. J. Thexton, K. M. Hiiemae, and A. W. Crompton, "Food consistency and bite size as regulators of jaw movement during feeding in the cat," *J Neurophysiol.*, vol. 44, no. 3, pp. 456–474, 1980.

[2] D. Yao, K. Yamamura, N. Narita, R. E. Martin, G. M. Murray, and B. J. Sessle, "Neuronal activity patterns in primate primary motor cortex related to trained or semiautomatic jaw and tongue movements," *Journal of Neurophysiology*, vol. 87, no. 5, pp. 2531–2541, 2002.

[3] K. Yamamura, N. Narita, D. Yao, R.E. Martin, Y. Masuda, and B.J. Sessle, "Effects of reversible bilateral inactivation of face primary motor cortex on mastication and swallowing," *Brain Res.*, vol. 944, no. 1-2, pp. 40 – 55, 2002.

[4] D. A. Reed and C. F. Ross, "The influence of food material properties on jaw kinematics in the primate, cebus," *Arch Oral Biol.*, vol. 55, no. 12, pp. 946 – 962, 2010.

[5] J. Iriarte-Díaz, D. A. Reed, and C. F. Ross, "Sources of variance in temporal and spatial aspects of jaw kinematics in two species of primates feeding on foods of different properties," *Integr Comp Biol.*, vol. 51, no. 2, pp. 307–319, 2011.

[6] C. Vargas-Irwin and J.P. Donoghue, "Automated spike sorting using density grid contour clustering and subtractive waveform decomposition," *J Neurosci Methods.*, vol. 164, no. 1, pp. 1 – 18, 2007.

[7] D. Daley and D. Vere-Jones, *An Introduction to the Theory of Point Process*, Springer-Verlag, New York, 2003.

[8] E. N. Brown, R. Barbieri, U. T. Eden, and L. M. Frank, *Computational Neuroscience: A Comprehensive Approach*, vol. 649, chapter Likelihood methods for neural spike train data analysis, pp. 253–286, CRC, 2003.

[9] W. Truccolo, U. T. Eden, M. R. Fellows, J. P. Donoghue, and E. N. Brown, "A point process framework for relating neural spiking activity to spiking history, neural ensemble, and extrinsic covariate effects," *J Neurophysiol.*, vol. 93, no. 2, pp. 1074–1089, 2005.

[10] H. Akaike, "A new look at the statistical model identification," *IEEE Trans Automat Contr*, vol. 19, no. 6, pp. 716 – 723, dec 1974.

[11] K.P. Burnham and D.R. Anderson, *Model Selection and Inference: A Practical Information-Theoretic Approach*, Springer, 2nd edition, 2002.

[12] S. Kim, D. Putrino, S. Ghosh, and E. N. Brown, "A granger causality measure for point process models of ensemble neural spiking activity," *PLoS Comput Biol*, vol. 7, no. 3, pp. e1001110, 03 2011.

[13] C. Granger, "Investigating causal relations by econometric models and cross-spectral methods," *Econometrica*, vol. 37, pp. 424–438, 1969.

[14] K. Sanggyun and E.N. Brown, "A general statistical framework for assessing granger causality," in *Conf. Proc. ICASSP*, mar 2010, pp. 2222 –2225.

[15] A. Dobson, *An introduction to generalized linear model*, CRC Press, 2002.

[16] Y. Pawitan, *In all likelihood: statistical modeling and inference using likelihood*, Oxford University Press, New York, 2001.

[17] M. E. J. Newman, *Networks: An introduction*, Oxford University Press, New York, 2010.

[18] S. Kim, K. Takahashi, N. G. Hatsopoulos, and T. P. Coleman, "Information transfer between neurons in the motor cortex triggered by visual cues," in *Conf Proc IEEE Eng Med Biol Soc*, Aug.30-Sep. 3 2011, pp. 7278 –7281.

[19] A. Thexton and K.M. Hiiemae, "The effect of food consistency upon jaw movement in the macaque: A cineradiographic study," *J Dent Res.*, vol. 76, no. 1, pp. 552–560, 1997.